JOURNAL OF MATERIALS SCIENCE 29 (1994) 965–972

Effect of annealing upon decomposition of electrodeposited iron–zinc alloy coatings

C. A. DREWIEN, A. R. MARDER
Materials Science and Engineering Department, Lehigh University, Bethlehem, PA 18015, USA

As-deposited electrodeposited iron–zinc alloy coatings containing η phase, decompose upon heating through a sequence of metastable phases. The hcp η phase transforms to bcc G, or Γ-like phase via a rapid diffusional phase transformation in the vicinity of 150 °C. For bulk iron contents of 8–13 wt %, η transforms to 100% G phase. The G phase subsequently transforms at 240 °C to ζ′ phase, which in turn transforms to δ or Γ_1 phase near 300 °C by depletion of iron from the surrounding matrix. The decomposition process may be driven by supersaturation of η with iron.

1. Introduction

The codeposition of iron and zinc from a sulphate-based or chloride-based electrodeposition cell has been developed for commercial processing of coated sheet steel. Electrodeposited iron–zinc alloy (EZA) coatings are applied to steel sheet used for automotive body panels, because they provide both galvanic and barrier corrosion resistance to the underlying steel. In addition to corrosion resistance [1], the properties of as-deposited EZA coatings, such as formability [2], weldability [3], and paintability [4], have been reported as a function of iron content for coatings produced from sulphate-based baths. Coatings that contain 8–18 wt % bulk iron exhibited optimized properties for automotive applications.

Although extensive structure/property relationship studies do not exist in the literature, the phase constitution of coatings has been evaluated as a function of iron content [2, 3, 5–7], and the coatings are known to contain nanocrystalline grain sizes [8]. Non-equilibrium phases, which are iron deficient or oversaturated with iron compared to the equilibrium phases of the iron-zinc binary system, comprised the microstructure of the coatings [3, 5]. An η phase, zinc supersaturated with iron, was reported in coatings with iron contents of 20 wt % or less. The η phase was hexagonal close-packed in structure; its lattice parameter changed continuously with iron content up to 8 wt % [5]. Reports on the δ and Γ phases varied. Some investigators claimed the δ phase was present [3] as the main phase for iron contents ranging from 13–20 wt %; δ phase first appeared at iron contents greater than 10 wt % and remained in the coating until the iron content exceeded 28 wt% [2]. Another study [6] based upon Mössbauer spectroscopy, X-ray diffraction, and TEM suggested that the δ phase did not exist in EZA coatings. Instead the phase observed was similar, but not exact, in structure to the Γ phase. This Γ-like phase was the main phase for iron contents ranging from 20–40 wt %. At higher iron contents, X-ray and selected-area diffraction patterns contained reflections that corresponded to interplanar spacings of 0.2178 and 0.207 nm. Although these interplanar spacings may be indexed as δ reflections, they probably belong to the Γ_1 phase [5]. The α phase was reported for iron contents greater than 50 wt %. In all these investigations, the ζ phase was not reported.

Some of the discrepancies between the reports of phase constitution may result from the electrodeposition processing technique; that is, different electrolytes and parameters were used in many of the studies. Crystal structures were not totally dependent upon iron content, and some influence of bath composition and plating conditions has been detected [9]. However, it should be noted that the X-ray diffraction patterns for the various intermetallic phases are very similar and that preferred orientation is prevalent in the coatings [10]. Therefore, the results that relied solely upon X-ray diffraction analysis may not be accurate or may be subject to differing interpretation. Table I summarizes the above observations and methods of detection. These reports are based upon studies of coatings produced from sulphate-based electrodeposition baths. No reports in the literature are available for coatings produced from chloride-based baths.

Based upon the presence of non-equilibrium phases, the stability of the microstructure of EZA coatings during a paint bake cycle (painted automotive body panels are cured at 175 °C for 30 min) is questionable. The transformation of the non-equilibrium, as-deposited structures towards equilibrium phases may occur with the application of heat. In fact, differential scanning calorimetry tests on EZA coatings containing 18.5 wt % Fe [7, 11] revealed exothermic reactions occurring at temperatures of 150, 210 and 300 °C. The reactions were attributed to the formation of δ, Γ_1, and Γ, respectively. Gu [12] showed that 11 and 18 wt % Fe EZA coatings transformed from as-deposited η and δ phases to equilibrium phases when heated

0022–2461 © *1994 Chapman & Hall*

TABLE I Synopsis of EZA coating reports

	Adaniya *et al.* [3]	Kondo *et al.* [5]	Shima *et al.* [6]	Hara *et al.* [2]	Kimoto *et al.* [7]
Bath	Sulphate	Sulphate	Sulphate	Sulphate	Sulphate
η (wt % Fe)	0–18	0–28	0–17	0–13	0–17
δ (wt % Fe)	12–28	No	No	10–28	7–27
Γ_1 (wt % Fe)	No	23–40	No	No	12–35
Γ (wt % Fe)	14–50	11–57	18.5–40	> 10	> 20
α (w/o Fe)	40–100	40–100	50–100	No	No
pH	2	1.5	2–3	3	1.8
Temp. (°C)	40	50	N/A	50	50
Flow rate ($m\,s^{-1}$)	1–3	13.3 r.p.s	1.5–2	1	N/A
Current density ($A\,dm^{-2}$)	10–50	80	50–60	50	50
Method of detection	X-ray	X-ray TEM	X-ray Mössbauer TEM	X-ray	X-ray

to temperatures near 300 °C for times of 30 min or longer. Thus, an understanding of the alloying behaviour of EZA coatings is necessary, in order to understand the changes that may occur in the microstructure during subsequent processing of the coated automotive body panels.

In this study, the effect of rapid heat treatment upon the phase stability of as-deposited EZA coatings is determined in order to recommend the use of heat treatment for rapid in-line processing of a galvannealed iron–zinc coating. The coatings used in this study were processed using a chloride electrodeposition bath.

2. Experimental procedure

Electrodeposited iron–zinc alloy coatings that contained 6, 8, 10, or 13 wt % were produced from a chloride-based electrodeposition bath [13]. Commercial and laboratory coatings were obtained from Double Eagle Galvanizing in Dearborn, MI, and from US Steel Corporation in Monroeville, PA, respectively. These bulk iron contents in the coatings were chosen, because at equilibrium the 6 wt % Fe coating should consist entirely of the ζ phase, the 8 and 10 wt % Fe coatings should consist entirely of the δ phase, and the 13 wt % Fe coating should consist of both the δ and Γ_1 phases.

Heat treatment of the EZA coatings was performed using both isothermal and non-isothermal heating methods. Short-term isothermal heat treatment was performed on a Gleeble thermomechanical testing unit. Sheet steel coated with the EZA coatings were sectioned into 5 cm × 20 cm pieces and resistively heated. Heating rates between 100 °C min^{-1} and 1000 °C. s^{-1} were used to heat the samples from room temperature to peak temperatures of 125–400 °C. Samples were held at peak temperature for times of 0.5–600 s and then cooled to room temperature through a water-quench, through a 40 °C s^{-1} controlled cooling rate, or through air cooling (approximately 10 °C s^{-1}). Long-term isothermal heat treatments were performed using a vacuum box furnace. EZA coated sheet steel samples were heated to 300 °C for 5 days. Non-isothermal heat treatment was performed using a differential scanning calorimeter. Samples of EZA coating only, or EZA coating on steel substrates were heated at heating rates between 5 and 99 °C min^{-1} to 400 °C. Samples were first weighed to ± 1 mg. With the exception of long-term isothermal heat treatments, all heat treatments were performed in nitrogen gas in order to limit oxidation.

Samples were analysed by X-ray diffraction techniques for phase constitution; quantitative X-ray diffraction was performed using an external standard method [10]. Pure zinc powder was used as an external standard for the η phase; the Γ phase was used as a standard for the G phase. A pure standard of Γ phase was made by mixing 25 wt % Fe and 75 wt % Zn powder, pressing the powder into a pellet, and heating the pellet in vacuum at 1000 °C for 3 days. A final homogenizing heat treatment of 400 °C for 10 days was performed on the pellet after cooling from 1000 °C and grinding away any oxide scale. Triplicate measurements were made on mixtures of the external standards, comprised of 10, 25, 50, 75 and 100 vol % Γ phase. A calibration curve of actual amount of Γ versus the experimentally measured amount of Γ was plotted and used for determining the volume fraction of η and G phases in the coatings. The error in the volume fraction determination was ± 6% to ± 10% of the value measured. The values are reported as the average value of triplicate measurements for 6 and 13 wt % Fe coatings and single measurements for 8 and 10 wt % Fe coatings.

Chemical titration was used to determine the bulk iron content of the coatings before and after heat treatment. The coating and substrate were weighed, and then the coating was dissolved in a 10% sulphuric acid solution. The substrate was reweighed, and the coating weight was determined by difference. The solution containing the dissolved coating was titrated with a 0.02 N $KMnO_4$ solution until the endpoint was detected by colour change. A minimum of five measurements were taken on as-deposited coatings, so that the variation in as-deposited bulk iron content could be considered in the value of a heat-treated coating's iron content. Triplicate measurements of iron content were taken on heat-treated coatings. The values are reported as an average value with the error in measurement, variation in as-deposited iron content, and variation in measured iron content shown as error bars.

In order to assure that the coatings consisted of only iron and zinc, Auger electron spectroscopy and residual gas analyses were performed on coatings in order to establish the presence of additional elements. Within the limit of detection of these techniques, only hydrogen at 500 p.p.m was detected in the EZA coatings.

3. Results and discussion

3.1. As-deposited coatings

The composition and crystal structure of as-deposited EZA coatings produced from a chloride-based electrodeposition bath were determined by chemical titration and X-ray diffraction analysis, respectively. As-deposited EZA coatings, containing 6, 8, 10, and 13 wt % bulk iron, were comprised of η phase with a minor amount of a Γ-like or G phase in the 10 and 13 wt % Fe coatings. The volume fractions of each phase, determined by quantitative X-ray diffraction analysis, and the experimentally determined iron content are presented in Table II. As with coating produced from sulphate-based electrodeposition baths, as-deposited η phase was supersaturated with iron to at least 8–9 wt%.

3.2. Heat-treated coatings

The thermal stability of the non-equilibrium, as deposited EZA coatings was determined using both non-isothermal and isothermal heat treatments. Continuous heating of 6, 8, 10 and 13 wt % iron EZA coatings at heating rates of 5–99 °C min^{-1} led to phase transformations from the as-deposited η phase towards more equilibrium structures. The thermal changes occurring in the coatings were monitored by power-compensated differential scanning calorimetry (DSC) in order to determine the temperatures of transition; exothermic peaks were observed near 150, 240 and 310 °C (see Fig. 1). X-ray diffraction analyses revealed that the peak at 150 °C represented the change from the η phase to the G phase; the peak at 240 °C corresponded to the transformation of the G phase to an intermediate ζ phase, which has be referred to as the pseudo-ζ, or ζ', phase [14]; and, the final peak represented the transformation from pseudo-ζ to the δ phase or to the Γ_1 phase, based upon iron content in the coating. The 6 and 8 wt % Fe coatings transformed to G phase, but did not show a considerable peak for the transformation to ζ'. They transformed to δ phase at approximately 300 °C. The 10 wt % Fe coatings transformed first to G, then to ζ', and finally to δ. The 13 wt % Fe coatings transformed to G phase and then to ζ', but did not transform to δ phase. They transformed instead to the Γ_1 phase at a temperature near 310 °C. The thermal profiles for all iron content coatings without the substrate are provided in Fig. 1a. The samples were heated at a rate of 90 °C min^{-1}. The sequence of transformations is provided schematically in Fig. 1b.

TABLE II As-deposited coatings; iron content and phase constitution

Processing technique	Iron content (± 2.5%)	Phase constitution (vol %)	
		η	G
Laboratory	6.15	100	
	8.4	100	
	10.05	99 +	Trace
	12.9	99 +	Trace
Commercial	5.8	100	
	7.8	100	
	10.3	99 +	Trace
	13.1	84	16

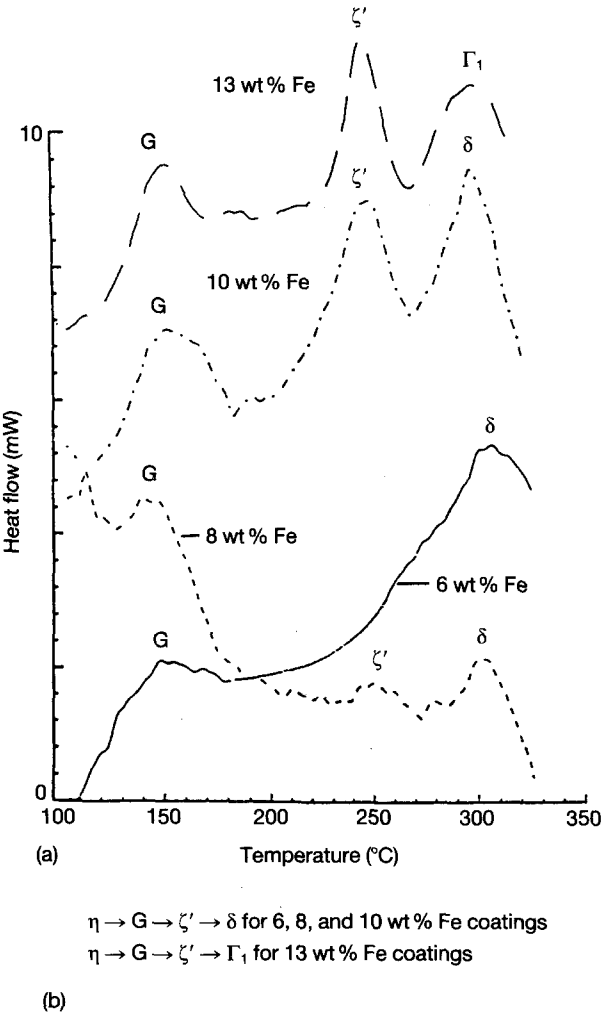

Figure 1(a) Differential scanning calorimetry profiles obtained on heating at 90 °C min^{-1} (i) 6 wt % Fe, (ii) 8 wt % Fe, (iii) 10 wt % Fe, and (iv) 13 wt % Fe EZA coatings. (b) Sequence of transformations detected in EZA coatings.

The transformation sequence was identical for commercial and laboratory coatings and for coatings with or without the substrate. When the substrate was not present, further heating led to an endothermic peak at the melting point of zinc. The melting point occurred at 419 °C regardless of the iron content in the coating, suggesting that solid solution effects were negligible and/or that formation of intermediate phases was complete. With the substrate intact, the same transformations occurred when a 90 °C min^{-1} heating rate was used; but, the endothermic peak of melting was considerably truncated as rapid liquid-phase diffusion gave rise to formation of intermediate phases of iron

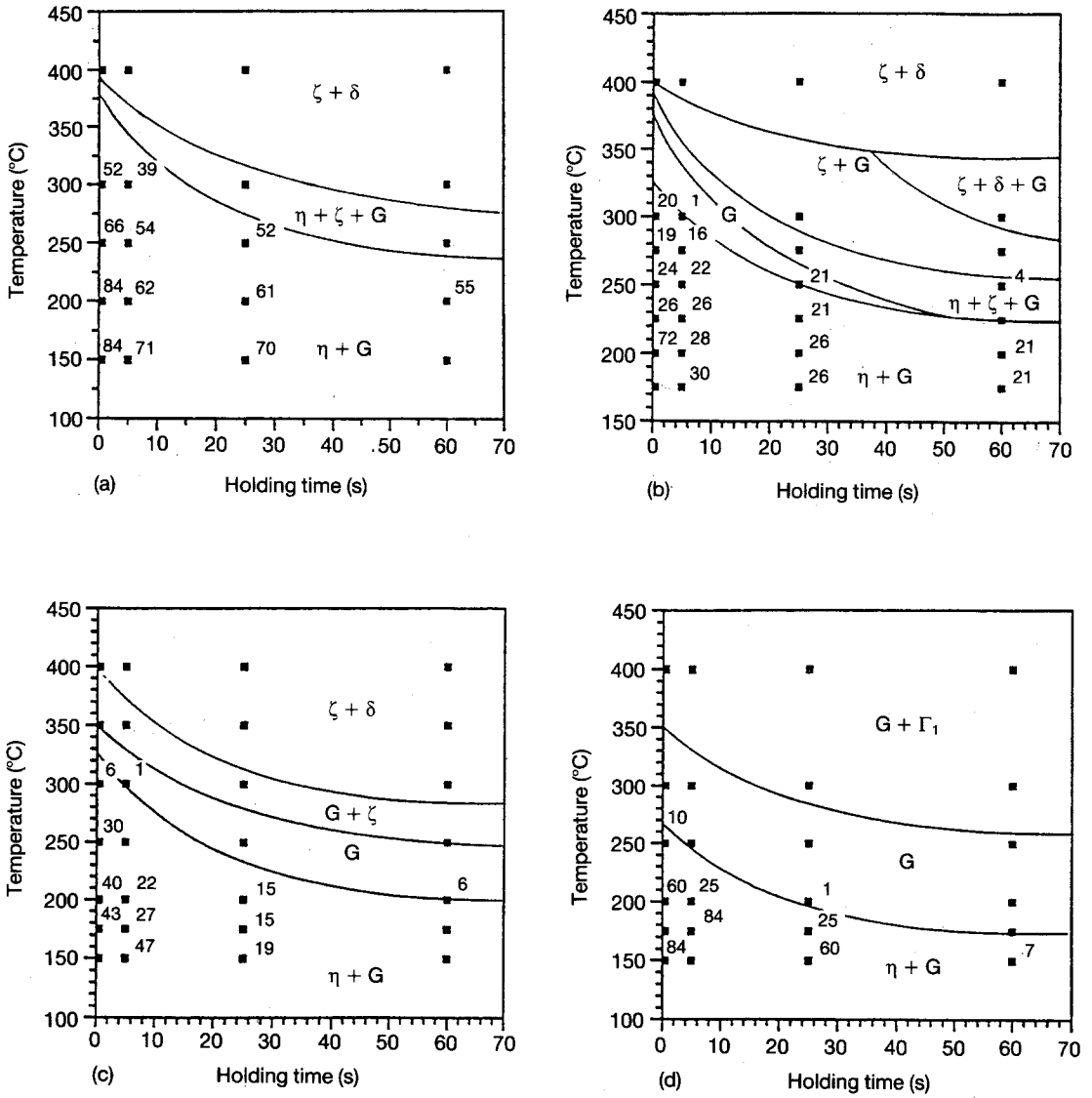

Figure 2 Time–temperature–transformation curves for heat treatment of (a) 6 wt % Fe, (b) 8 wt % Fe, (c) 10 wt % Fe, and (d) 13 wt % Fe commercial EZA coatings show phase fields for G, pseudo-ζ, δ, and Γ_1 phases. Heating rate 100 °C s^{-1}

and zinc, due to interaction of the coating with the substrate.

Time–temperature–transformation curves from isothermal heat treatment of commercial EZA coatings using the Gleeble thermomechanical testing unit are shown in Fig. 2. The numbers in the phase fields containing η indicate the volume fraction of η phase determined by quantitative X-ray diffraction analysis. Boundaries between η, G, ζ′, δ, and Γ_1 phases were estimated from X-ray diffraction analysis. The TTT curves indicated that the higher iron content coatings transformed from η to G phase more rapidly than lower iron content coatings. This can be seen by comparing the volume fraction of η phase for a 6 wt % Fe EZA coating heated at 100 °C s^{-1} to 250 °C for 0.5 s with that for a 13 wt % Fe EZA coating (66 vol % η phase was detected in the 6 wt % Fe coatings while 10 vol % η phase was detected in the 13 wt % Fe coatings). A higher driving force for transformation may be achieved by the greater supersaturation of η with iron or by the greater amount of strain present in η due to a greater amount of iron present.

As with non-isothermal heating, G, ζ′, and δ or Γ_1 phases were detected in heat-treated EZA coatings; however, no pseudo-ζ phase field was detected for the 13 wt % Fe coatings. Instead, a large G phase field followed by a Γ_1 field was detected. The discrepancy could arise for a variety of reasons:

(i) large time or temperature increments in isothermal heating obscured detection of ζ′;

(ii) the ζ′ phase formed in insufficient quantities, so that it was not detected by X-ray diffraction analysis; or

(iii) strain from non-isothermal heating produced varied nucleation sites that gave rise to the formation of ζ′ during non-isothermal heat treatment, but not during isothermal heat treatment.

The transformation sequence was otherwise in excellent agreement between isothermal and non-isothermal heat treatment.

Despite the rapid heat treatment and quench cycle, time–temperature–transformation curves suggested that longer hold times or higher peak temperatures gave rise to more of the second phase. After heating a

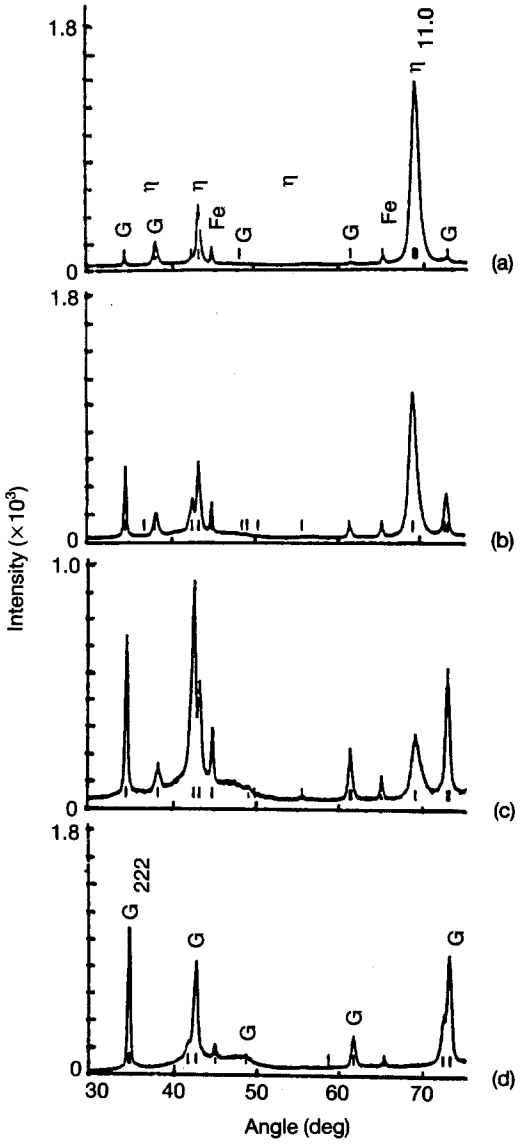

Figure 3 X-ray diffraction patterns of 10 wt % Fe commercial EZA coatings heated at 100 °C, held at temperature for (a) 0.5 s, (b) 5 s, (c) 25 s, and (d) 60 s, then quenched to room temperature with water.

6 wt % Fe coating at 100 °C s^{-1} to 150 °C for 5 s, 71 vol % η phase was detected, while 39 vol % η phase was obtained when the coating was heated to 300 °C for 5 s. A time–temperature dependent transformation is shown in Fig. 3, which presents the X-ray diffraction patterns for a 10 wt % Fe EZA coating heated at 100 °C s^{-1} to 150 °C for 0.5, 5, 25, and 60 s, then quenched to room temperature. The decrease in intensity of the {11.0} planes of the η phase coincided with the emergence of the {222} planes of the G phase.

In order to show further that diffusional transformations existed, the influence of heating and cooling rates upon the η to G transformation was tested. Heating at varied rates produced a difference in the amount of second-phase formation. As an example, a 13 wt % Fe coating heated to 200 °C and held for 0.5 s before cooling yielded 20 vol % G phase when a heating rate of 1000 °C s^{-1} was used and 40 vol % G phase when a heating rate of 100 °C s^{-1} was used. Alternately, slower cooling rates, achieved through lower pressure water–air quenches and through air

TABLE III Effect of heating and cooling rate on amount of G formed in 13 wt % Fe commercial EZA coatings heated to 200 °C for 0.5 s

Heating rate (°C)	Cooling rate (°C)	η(%)	G(%)	Iron content (wt % Fe)
1000	Quench	80	20	12.77
400	Quench	80	20	13.09
200	Quench	74	26	13.12
100	Quench	60	40	12.67
	40	22	78	12.99
	Air cool	12	88	13.4
16.7	Quench	11	89	13.95
	Air cool	–	100	15.79
1.67	Quench	–	100	14.2
	40	–	100	14.44

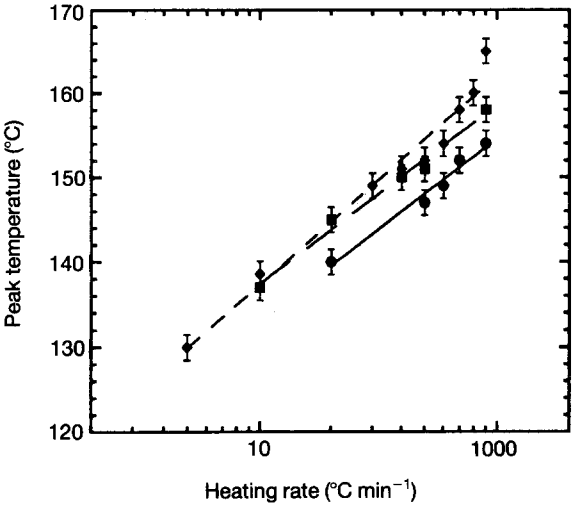

Figure 4 Temperature at which rate of formation of G phase is maximum as a function of heating rate shows an increasing relationship. (– ● –) 8 wt % Fe, (– ■ –) 10 wt % Fe, (– – ◆ – –) 13 wt % Fe.

cooling, produced more G phase when the heating rate, peak temperature, and hold time were held constant. This information is presented in Table III, which contains the volume fraction of η and G phases found in heat-treated 13 wt % Fe commercial coatings.

The change in peak temperature of transformation with constant heating rate, as used in the DSC tests, also provided an indication of diffusional phase transformations. The peak temperature of transformation, or T_{max}, was determined from DSC data as a function of heating rate. The results for the η to G phase transformation are shown in Fig. 4 for 8, 10, and 13 wt % Fe laboratory EZA coatings. The temperature of maximum transformation rate, T_{max}, increased with increased heating rate for all exothermic phase transformations detected in the EZA coatings. In accordance with a time and temperature dependence, the temperature at which the maximum amount of material transformed increases with increased heating rate, because the shorter heating cycle required higher temperatures in order to transform the same amount of material.

The results from heat treatment of as-deposited EZA coatings produced from chloride-based elec-

trodeposition baths were similar to results from studies on coatings produced from sulphate baths, except that the identification of some phases varied. The difference between findings by Kimoto *et al.* [7] and the findings of this study might be explained by a difference in iron content or phase constitution in the as-deposited coatings. However, it is possible that the difference arose due to interpretation of the X-ray diffraction patterns. Several peaks of the G phase were close in proximity to those of the δ phase. The consistent analysis of the diffraction patterns from incremental heat treatments, as performed in the present study, provided a better basis for determining if the presence of a peak corresponded to G phase or δ phase. The peaks corresponded to a bcc phase, similar to equilibrium Γ phase. The detection of the G, or Γ-like, phase agreed with that found by Kondo *et al.* [5].

The phases that formed during heat treatment of EZA coatings were analysed in terms of iron content and crystallography. The iron contents of isothermally heat-treated EZA coatings, measured using chemical titration, are shown in Fig. 5. For temperatures less than 300 °C and times of 25 s or less, no change in iron content was detected even though the coatings had undergone phase transformations from the as-deposited structure to G and ζ′ phases. In that 100 vol % G phase was detected in some 8, 10, and 13 wt % Fe content coatings, the G phase contained 8, 10, or

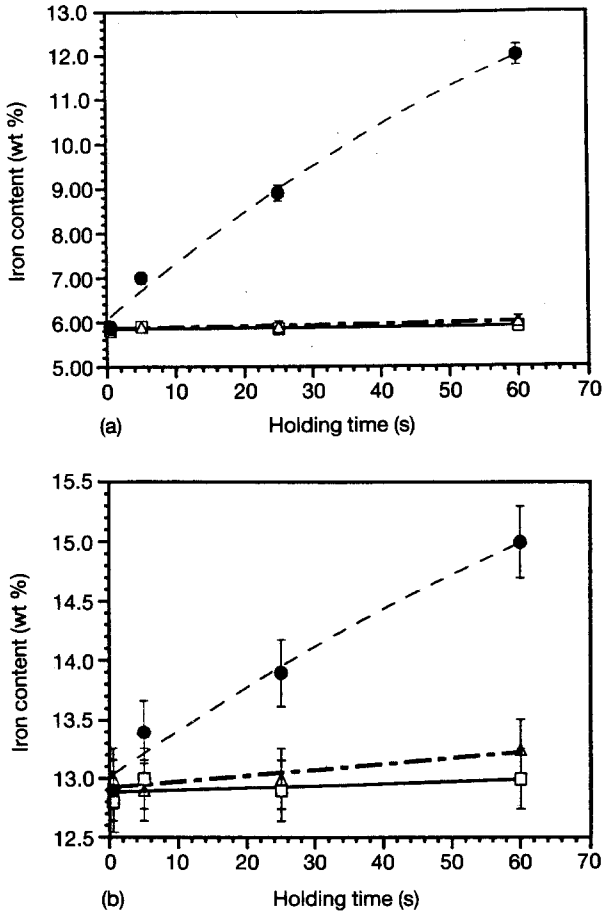

Figure 5 Change in iron content with heat treatment of (a) 6 wt % and (b) 13 wt % Fe commercial EZA coatings shows that iron content increases only after heating at 300 °C for 25 s or greater. (– □ –) 200 °C, (– △ –) 300 °C, (– – ● – –) 400 °C.

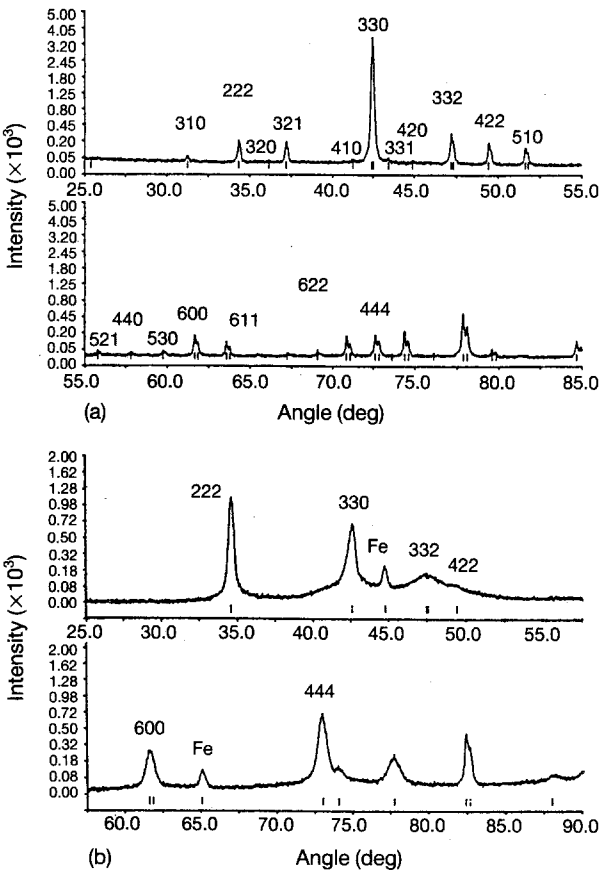

Figure 6 X-ray diffraction patterns of (a) Γ and (b) G phase illustrating differences between equilibrium and non-equilibrium phases.

13 wt % Fe. Because quantification of ζ′ was not attempted, the actual iron content of this phase is unknown. Reports in literature [14] place the iron content of the ζ′ phase in the region of 5.8–10 wt %. This amount of iron could easily exist in the ζ′phase detected here. When δ or Γ_1 was detected in the X-ray diffraction patterns, an increase in iron content of the coatings was observed, compare data in Fig. 2 with data in Fig. 5.

The crystallography of the phases was determined by X-ray diffraction analysis. The X-ray diffraction patterns of G phase revealed a bcc structure whose lattice parameter (0.899 nm) was identical to that of Γ. However, the G phase was not the equilibrium Γ phase. Its diffraction pattern differed from the pattern of Γ, and the G phase contained less iron than equilibrium Γ. In order to illustrate the difference between G and equilibrium Γ phase, the diffraction patterns are provided in Fig. 6a and b, respectively. The G phase diffraction pattern lacked the superlattice reflections ({320}, {410}, {331}, {421}, {500}. etc.) present in the profile of the Γ phase, and G phase peaks were very broad.

Similarly, the pseudo-ζ phase differed from the equilibrium ζ phase, because it lacked intensity in the {331} planes compared to the equilibrium ζ phase. Unfortunately, a diffraction pattern of 100 vol % ζ′ phase was not obtained and the difference cannot be illustrated. No difference between the equilibrium δ and Γ_1 phases and the δ or Γ_1 phases obtained here could be detected due to the overlap of peaks from other phases in the EZA coatings.

Therefore, the phases detected in the rapidly heat-treated coatings were not the equilibrium phases of the iron–zinc binary system. In an effort to establish the equilibrium phases predicted by the iron–zinc binary phase diagram, coatings were isothermally heated at 300 °C for 5 days in vacuum box furnace. After heat treatment, the coatings were analysed by X-ray diffraction analysis. The 6 wt % Fe coatings contained equilibrium ζ and δ phases when heated at 300 °C for 5 days. Some loss of zinc by evaporation may have allowed the formation of the higher iron content phase, δ. The final iron content was 6.8 wt %. The 8 and 10 wt % Fe EZA coatings were comprised entirely of δ phase, as predicted by the equilibrium iron–zinc phase diagram; and, the 13 wt % Fe EZA coatings transformed to δ and Γ_1 phases (again the phases predicted under equilibrium at 300 °C). Similar results were found by Gu [12]; long heat-treatment times brought about the formation of equilibrium iron–zinc intermetallic phases.

The formation of the metastable G and ζ' phases can be explained from a qualitative approach to the kinetics, driving force, and activation energy for transformation. The difference in free energy between the as-deposited 10 wt % Fe η phase coating (see the schematic free-energy diagram in Fig. 7) and the free energy of the G phase, ΔG^*, is the driving force for transformation from η to G phase, while the difference in free energy between as-deposited 10 wt % Fe η and the free energy for the thermodynamically equilibrium phase at room temperature, the δ phase, $\Delta G^* + \Delta G_e$, provides the driving force for the transformation from η phase to δ phase. Note that the driving force for the transformation from η to δ phase is greater than that for the transformation from η to G phase. The activation energy for transformation must first be supplied; the activation energy represents the competition between the driving force for transformation and the barriers to nucleation of the product phase. If the activation energy is achieved, the transformation to the product phase occurs. However, once the activation energy is met, the transformation is then controlled by the kinetics of transformation, including the nucleation and growth processes for the product phase. Given that the 10 wt % Fe η phase coatings transformed to G phase in spite of the greater driving force for transformation to the δ phase, (i) the activation energy for formation of δ phase was either not achieved, or (ii) the nucleation and growth processes for transformation to G phase were more rapid than those for transformation to the δ phase.

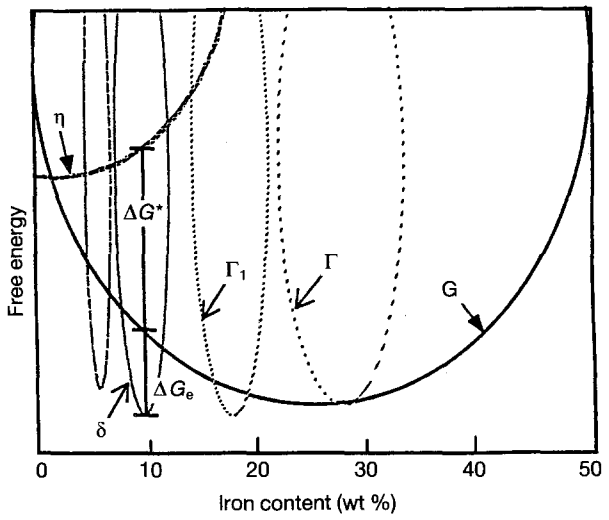

Figure 7 Free energy of as-deposited 10 wt % Fe EZA coating decreases with formation of G phase from η phase. ΔG^*, driving force for η to G; $\Delta G_e + \Delta G^*$, driving force for η to equilibrium δ.

4. Conclusion

The in-line galvannealing of electrodeposited iron–zinc alloy coatings is possible by rapid heating techniques. Phase formation during heat treatment of EZA coatings with 6–13 wt % Fe occurred via decomposition process, followed by equilibrium phase formation. The decomposition of as-deposited η phase occurred through a sequence of metastable transitional phase formation. The iron-supersaturated hcp η phase transforms completely near 150 °C to an iron-deficient bcc Γ-like or G phase in 8, 10, and 13 wt % Fe coatings. The transformation is a diffusional transformation, occurring entirely within the coatings. The same transformation occurred in laboratory and commercial coatings. The 6 wt % Fe coatings did not transform completely to G phase but retained η phase in their microstructure. The G phase subsequently transformed to ζ' phase at 240 °C and then δ or Γ_1 phase near 300 °C by depletion of iron from the surrounding matrix, which became enriched in zinc such that an endothermic peak is encountered at the melting point of pure zinc. For longer heat-treatment times at 300 °C, equilibrium phases formed in the electrodeposited iron–zinc coatings.

Evidently, supersaturation of η phase with iron provided a sufficient driving force for transformation to G. The nucleation and growth processes of G phase are more rapid than those of the equilibrium phases, as demonstrated by the rapid transformation to the metastable phases.

Acknowledgements

The authors acknowledge the financial support of the International Lead and Zinc Research Organization, Lepel Corporation, Rouge Steel, and Kobe Steel. The samples were generously donated by Double Eagle Galvanizing Line and US Steel Corporation. The authors thank Dr F. E. Goodwin, Dr M. Gu, Dr C. J. Wu, Mr J. Manack, Mr B. Cowell, and Mr G. Yasko for their individual contributions to the study.

References

1. T. ADANIYA, Y. HARA, M. SAGIYAMA, T. WATANABE and T. HONMA, in "Surface Modification and Coatings", edited by R. D. Sisson (ASM, Metals Park, OH, 1986) p. 1.
2. T. HARA, T. ADANIYA, M. SAGIYAMA, T. HONMA, A. TONOUCHI, T. WATANABE and M. OHMURA, *Trans. ISIJ* **23** (1983) 954.
3. T. ADANIYA, Y. HARA, M. SAGIYAMA, T. HONMA and T. WATANABE, *Plating Surface Finishing* **72** (1985) 52.
4. S. WAKANO, A. SAKODA, M. NISHIHARA, T. KURIMOTO and Y. HOBOH, in "Surface Modifications and Coatings", edited by R. D. Sisson (ASM, Metals Park, OH, 1986) p. 23.

5. K. KONDO, S. HINOTANI and Y. OHMORI, *J. Appl. Electrochem.* **18** (1988) 154.
6. Y. SHIMA, M. TERASAKA, K. NAKAOKA, T. HARA and T. HONMA, *Tetsu to Hagane* **72** (1986) 66.
7. M. KIMOTO, S. WAKANO and A. SHIBUYA, *ibid.* **72** (1986) 73.
8. M. GU, M. R. NOTIS and A. R. MARDER, in "Proceedings of the International Conference on Zinc and Zinc Alloy Coated Steel Sheet", edited by Y. Hisamatsu, Galvatech '89, Keidanren Kaikan, Tokyo, Japan 5–7 September (1989), pp. 462–77.
9. T. WATANABE, M. OHMURA, T. HONMA and T. ADANIYA, SAE Techn. Paper 820424, Warrendale, PA (1982).
10. M. GU and A. R. MARDER, *Powder Diff.* **6** (2) (1991) 89.
11. Y. TOKUNGA and M. YAMADA, *Trans. ISIJ* (1984) 97.
12. M. GU, Ph D dissertation, Lehigh University, Bethlehem, PA (1989)
13. W. R. JOHNSON and L. E. PFISTER, US Pat. 4540472, *Official Gazette* (1985) 768.
14. M. ONISHI, Y. WAKAMATSU and H. MIURA *Trans. JIM* **15** (1974) 331.

Received 1 December 1992
and accepted 12 May 1993